

Fluorescent Probes

A Pro-Fluorescent Ubiquitin-Based Probe to Monitor Cysteine-Based E3 Ligase Activity

David A. Pérez Berrocal, Thimmalapura M. Vishwanatha, Daniel Horn-Ghetko, J. Josephine Botsch, Laura A. Hehl, Sebastian Kostrhon, Mohit Misra, Ivan Đikić, Paul P. Geurink, Hans van Dam, Brenda A. Schulman, and Monique P. C. Mulder*

In memory of Professor Huib Ovaa, his passion for science will always be an inspiration to us.

Abstract: Protein post-translational modification with ubiquitin (Ub) is a versatile signal regulating almost all aspects of cell biology, and an increasing range of diseases is associated with impaired Ub modification. In this light, the Ub system offers an attractive, yet underexplored route to the development of novel targeted treatments. A promising strategy for small molecule intervention is posed by the final components of the enzymatic ubiquitination cascade, E3 ligases, as they determine the specificity of the protein ubiquitination pathway. Here, we present UbSRhodol, an autoimmolative Ub-based probe, which upon E3 processing liberates the pro-fluorescent dye, amenable to profile the E3 transthiolation activity for recombinant and in cell-extract E3 ligases. UbSRhodol enabled detection of changes in transthiolation efficacy evoked by enzyme key point mutations or conformational changes, and offers an excellent assay reagent amenable to a high-throughput screening setup allowing the identification of small molecules modulating E3 activity.

Introduction

Ubiquitination constitutes one of the most versatile and dynamic post-translational modification pathways in eukaryotes.^[1] ATP-dependent reversible covalent attachment of ubiquitin (Ub), a 76 amino acid protein, to, in most cases, a lysine residue on protein substrates,^[1a,2] yields a vast cellular signalling network pivotal in a myriad of biological processes.^[3] A vast number of possible combinations of Ub patterns decorating a substrate protein can be formed, generating a complex and dynamic Ub code.^[1b] The state of this code is controlled by both the writers (E1–E2–E3 enzymes) responsible for ubiquitination and the erasers (deubiquitinases (DUBs)) that reverse or modify it. The encoded message in the generated Ub chains serves as a beacon to exert a plethora of biological functions including protein homeostasis, cell cycle progression, and regulation of DNA integrity.^[1b] The actions of writers and erasers are tightly coupled and the balance between ubiquitination and deubiquitination is a critical determinant of protein levels and activity. It is not surprising that aberrant functioning of this finely tuned system is implicated in numerous diseases, including neurodegeneration, cancer, autoimmune and metabolic diseases.^[4] In this light, the Ub system offers an attractive, yet underexplored route to the development of novel targeted treatments and recent studies have shown the feasibility and complexity of targeting the Ub system for drug intervention.^[5]

Given the hierarchical nature of Ub signaling, E3 ligases are of particular interest as they determine the specificity of the ubiquitination system by recognizing, discriminating, and interacting with the proper protein substrate thereby regulating its stability and functioning.^[6] Drugs targeting the activity of a particular E3 ligase are therefore expected to offer one of the most specific and powerful approaches for therapeutic intervention within the ubiquitination cascade.^[7] Traditionally, E3 inhibitor screening relied on entire E1–E2–E3 cascade assays,^[8] due to the intrinsic multi-step nature of the system, which made the methodology not amenable for high-throughput formats.^[9] Recently, however, simplified reconstitution systems have been reported, in which Ub is chemically activated as a thioester thereby allowing its reaction with the catalytic cysteine of E3 ligases in the absence of ATP, and E1 and E2 enzymes.^[10] Here, we

[*] D. A. Pérez Berrocal, Dr. T. M. Vishwanatha, Dr. P. P. Geurink, Dr. H. van Dam, Dr. M. P. C. Mulder
Department of Cell and Chemical Biology, Leiden University Medical Center (LUMC)
Eindhovenweg 20, 2333ZC Leiden (The Netherlands)
E-mail: m.p.c.mulder@lumc.nl

Dr. D. Horn-Ghetko, J. J. Botsch, L. A. Hehl, Dr. S. Kostrhon, Prof. Dr. B. A. Schulman
Department of Molecular Machines and Signaling, Max Planck Institute of Biochemistry
Am Klopferspitz 18, 82152 Martinsried (Germany)

Dr. M. Misra, Prof. Dr. I. Đikić
Institute of Biochemistry II, Faculty of Medicine, Goethe University Theodor-Stern-Kai 7, 60590 Frankfurt am Main (Germany)

© 2023 The Authors. Angewandte Chemie International Edition published by Wiley-VCH GmbH. This is an open access article under the terms of the Creative Commons Attribution License, which permits use, distribution and reproduction in any medium, provided the original work is properly cited.

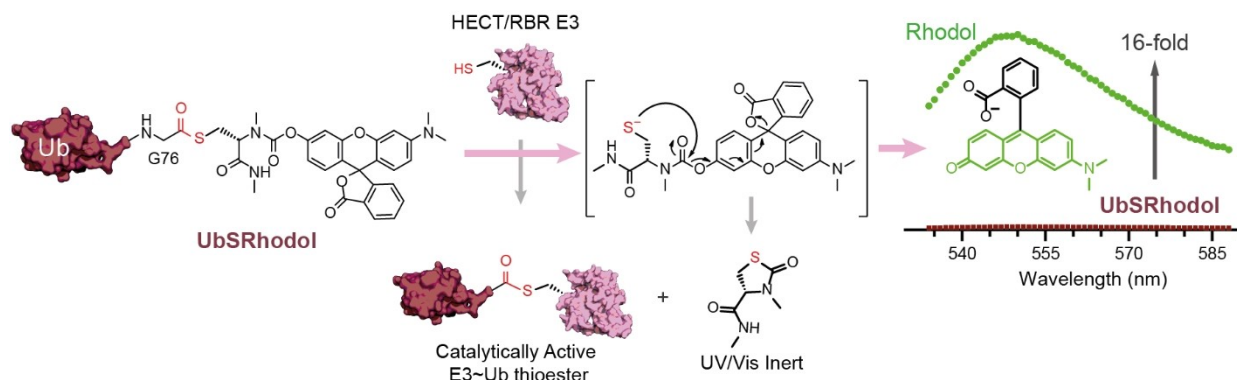


Figure 1. Mechanism of UbsRhodol. Ub equipped with a self-immolative fluorophore liberated after attack of the E3 ligase allows monitoring of the transthioylation reaction. Attack of the E3 ligase triggers an intramolecular cyclisation liberating an inert UV/Vis thiolazolidine-2-one while rearranging the Rhodol dye in its fluorescent state giving rise to a 16-fold fluorescence intensity increase (DTT was used as reducing agent to determine the FI fold increase). ($\lambda_{ex/em}$ 515/548 nm).

describe a sensitive high-throughput assay based on a synthetic pro-fluorescent Ub thioester (UbsRhodol) that allows quantitative analysis of changes in cysteine-based E3 ligase activity evoked by small molecules, biochemical mutations or conformational changes induced by protein-protein interactions.

UbsRhodol was synthesized by conjugating a glycine thioester bearing a pro-fluorescent molecule^[11] via a carbamate-thiol linker (**1**) to the C-terminus of Ub(1–75). The carbamate modification on Ub forces the rhodol fluorophore into the lactone form, which has very low fluorescence. This self-immolative fluorophore is liberated after a direct transthioylation reaction with the catalytic cysteine of the E3 ligase, producing the catalytically active E3~Ub thioester. Enzymatic release of the pro-fluorescent molecule liberates a cysteine-based linker which cyclizes rapidly, intramolecularly attacking the carbamate bond, thereby releasing a free Rhodol dye and concomitantly triggering a strong fluorescence signal (Figure 1). Importantly, where other assays such as fluorescence polarization (FP) readout is based on the ratio between bound and unbound fluorophore, requiring a large amount of substrate processed to have an acceptable window for the assay signal, our setup relies on unbound fluorophore only.

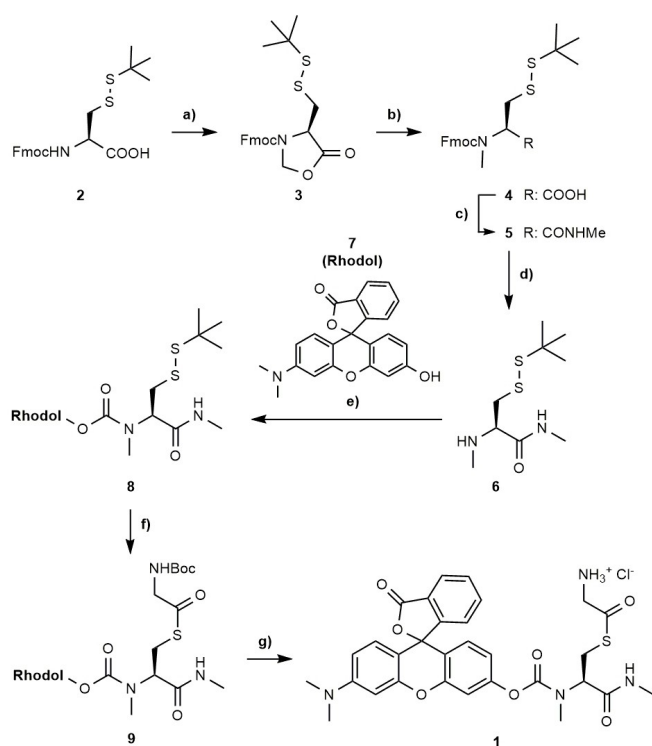
This setup allowed us to profile E3 ligase activities in real time, while the high sensitivity of the assay permits enzyme screening in the low nanomolar range, enabling screening of large libraries with minimal enzyme and reagent amounts. Thus far, we have profiled the activity of 9 HECTs and 5 RBR enzymes using this reagent, including assays for overexpressed ligases in total cell lysates, showing its ease of execution and facile translation from one E3 ligase to the next. Collectively, our UbsRhodol bypass system presents a potent screening platform for targeting and monitoring enzymatic activity, offering opportunities for drug discovery.

Results and Discussion

Chemical Synthesis of UbsRhodol

The synthesis of key building block **1** (Scheme 1) started from commercially available Fmoc-Cys(SStBu)-OH (**2**), which was converted to the corresponding oxazolidinone **3** by heating it to reflux in toluene with paraformaldehyde and catalytic amount of camphorsulfonic acid. Treatment of **3** with TFA:TES afforded Fmoc-MeCys(SStBu)-OH (**4**),^[12] which was coupled with methyl amine hydrochloride under standard peptide coupling conditions giving rise to amide **5**. Fmoc deprotection of **5** yielded the pro-autoimmolative linker **6**. Subsequently, Rhodol^[13] (**7**) was treated with triphosgene in presence of triethylamine and the resulting carbamoyl chloride reacted with the amine of cysteine derivative **6**, affording compound **8**. By use of THPP (Tris(3-hydroxypropyl)phosphine) as a reducing agent^[14] the reduction of the SStBu protecting group of derivative **8** was achieved within 20 min, after which the solution was acidified to pH 5.0, and followed by treatment with Boc-glycine acyl imidazole^[15] to obtain the carbamate-thiol precursor **9**. A final Boc deprotection carried out in 4 N HCl in dioxane, afforded key building block **1**.

UbsRhodol was synthesized on a 20 μ mol scale starting from Ub(1–75), using a previously reported linear Fmoc-based solid phase peptide synthesis (SPPS) of Ub,^[16] in which **1** was coupled to the C-terminal carboxyl group of protected Ub(1–75). Global deprotection with 90 % TFA and purification by HPLC gave the desired UbsRhodol in \approx 18 % overall yield. LC–MS analysis confirmed successful preparation of the compound in >95 % purity (Supporting Information Figure 1) The thioester proved stable both during synthesis and storage.



Scheme 1. Synthesis of building block **1**. Reagents and conditions:

a) (HCHO)_n, CSA (cat), toluene, reflux, 18 h, 92%; b) TFA, TES, CHCl₃, rt, 24 h, 85%; c) MeNH₂·HCl, HBTU/HOBt, DIPEA, CH₂Cl₂, 0 °C to rt, 12 h, 90%; d) DEA, ACN, rt, 1 h, 91%; e) i.) Triphosgene, TEA, THF, 0 °C, 30 min; ii.) **6**, THF, rt, 1 h, 28%; f) i.) THPP, THF:H₂O (9:2), rt, 30 min; ii.) Boc-Gly-Im, THF, rt, 1 h, 60%; g) 4 N HCl/dioxane, rt, 30 min, 98%.

Profiling Transthioation Activity

With the UbsRhodol reagent in hand we set out to confirm the cyclization and spectral properties of the self-immolative fluorophore. Incubation of UbsRhodol with the reducing agent DTT (0.001–5 mM) followed over time yielded the hydrolysis of the thioester (Supporting Information Figure 2), releasing the cysteine-based linker which cyclizes intramolecularly by attacking the carbamate bond, triggering a strong fluorescence signal (Figure 1). The formation of the liberated fluorophore was measured using a fluorescence photospectrometer ($\lambda_{\text{ex/em}}$ 515/548 nm, Figure 1 and Supporting Information Figure 3A, B), and a fluorescence intensity (FI) increase of 16-fold was observed. The Rhodol liberation and FI build-up can also be measured at the widely used rhodamine wavelength ($\lambda_{\text{ex/em}}$ 490/520 nm) with a comparable FI increase fold (Supporting Information Figure 3C). Having successfully demonstrated the intramolecular cyclization and release of the Rhodol in a general assay buffer at physiological pH (HEPES 50 mM, 150 mM NaCl, 1 mM TCEP, pH 7.5), we started to test the ability of UbsRhodol to measure E3 transthioation activity. Importantly, DTT has to be omitted in buffers for enzyme preparations as it affects thioester stability (Supporting Information Figure 2), instead TCEP can be used as reducing agent as it reduces

oxidized sulfhydryls and disulfides but has no effect on thioester stability.^[17]

The ability of UbsRhodol to measure E3 transthioation activity is dependent on the E3~Ub adduct formed and the easiness of its lysine-dependent discharge yielding a repertoire of Ub products with the bypass system (UbsR + E3) (Figure 2A). In short, the E3 catalytic cysteine attacks UbsRhodol at its thioester bond forming a new E3~Ub thioester, which can then discharge Ub onto a lysine either from the probe (unanchored Ub chain elongation pattern (I)), the E3 ligase itself (autoubiquitination pattern (II); a common phenomenon for E3s in *in vitro* assays), or from a cognate substrate (substrate ubiquitination (III)). These Ub products can be confirmed employing chemically synthesized fluorescently labelled bypass probes in gel-based assays (Supporting Information Figure 4A). When the newly formed E3~Ub adduct is discharged the E3 ligase will undergo multiple cycles increasing the window of the assay and this will considerably reduce the amount of E3 needed for an acceptable assay window. Moreover, by simply modifying the ratio of enzyme over probe, reactions can be run under single turnover conditions (ST, from excess to equimolar amount of E3) to measure transthioation rates, or under multi turnover conditions (MT, excess of probe) to observe the overall rate of Ub probe turnover and study both transthioation and ligation steps. This fluorescence intensity read-out is highly sensitive and allows to profile E3 transthioation activity in the low nanomolar range (Figure 2C).

We measured the transthioation profile of different cysteine-based E3 ligase members (Supporting Information Figure 5 and 6). In humans, the known thioester-forming E3s, which harbour a catalytic cysteine loaded with Ub by a mechanism analogous to the E1 and E2 enzymes, fall into the HECT^[18] (28 human family members) and RBR^[19] (13 human members) classes. Therefore, panels comprising different subfamilies within both the HECT class (9/28 E3s profiled, Supporting Information Figure 5) and RBR class (5/13 E3s profiled, Supporting Information Figure 6) were evaluated. For all enzymes a concentration and incubation time dependent processing of UbsRhodol was demonstrated.

As HECT E3 ligases are often very large, ranging from 700 amino acids to giant enzymes of more than 3000 residues (i.e. UBR5,^[20] HUWE1 and HERC1, 2798, 4374 and 4861 residues respectively), it can be a challenge to study them in biochemical studies. Strikingly, the isolated C-terminal HECT domain of UBR5, was still able to process UbsRhodol in a catalytic transthioation dependant manner (Supporting Information Figure 7A). Under similar conditions, gel-based experiments using chemically synthesized N-terminal rhodamine tagged Ub bypass probe (RhoUbsR) detects marginal thioester formation by fluorescent scanning (Supporting Information Figure 7B–C). Given the technical problems in reconstituting full-length HECT E3 enzymes of large HECT E3s, our sensitive readout opens the avenue of *in vitro* activity profiling of low reactive E3 ligases constructs.

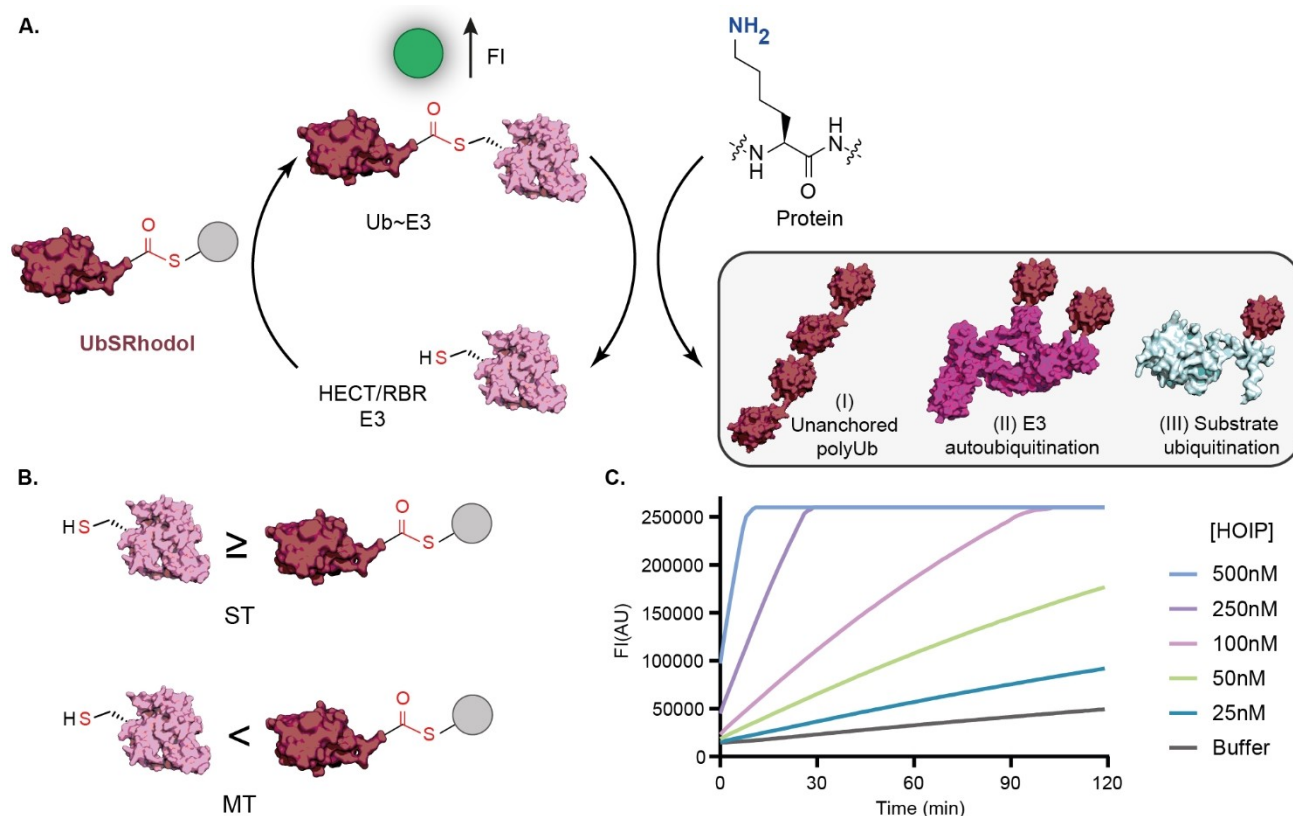


Figure 2. UbSRhodol assay set up. A) UbSRhodol is recognized by Ub-binding domains at the catalytic domain of HECT and RBR ligases, positioning the reactive thioester for transthiolation reaction and forming a Ub~E3 thioester adduct. Concomitantly, a molecule of Rhodol dye is liberated after rapid intramolecular cyclisation of the autoimmolative linker. If an acceptor lysine is present, and E3 favors ligation, different ubiquitination products can be generated: (I) Unanchored polyUb formation, (II) E3 autoubiquitination and (III) Substrate ubiquitination. B) Single turnover (ST) or Multi turnover (MT) conditions can be selected by altering the ratio of E3 over probe. In general, ST conditions are preferential to study transthiolation, while MT conditions are preferred to study both transthiolation and ligation. C) HOIP-dependent transthiolation of UbSRhodol in the low nanomolar range showcases sensitivity of the assay.

With this platform in hand, we evaluated the potential of our assay in measuring changes in ligase activity, caused by key point mutations. As the mode of action of HECT ligases is conserved through the different NEDD4 family members, with a high degree of homology in the HECT domain, a set of 14 representative mutants of the NEDD4L HECT domain were chosen. The point mutations can be sorted into different categories including the catalytic loop (H876A/E, T877A, F879A, N880A, C878A), the E2 binding site (Y692A and W698A/E), the C-lobe Ub binding site (L872A and M899A), the N-lobe Ub binding site (F718A), the -4F (F907A) and the acidic loop (D595A). The mutants are based on previous studies determining the reaction mechanism of HECT E3 ligases.^[21] All mutants were profiled using UbSRhodol to detect transthiolation and/or ligation defects (Figure 3A, Supporting Information Figure 8). As expected, the catalytically dead C878A mutant was not able to form isopeptide linkages, as corroborated by bypass probe gel-based assays in the presence of β -mercaptoethanol (β ME) (Supporting Information Figure 8). However, some residual activity was observed and therefore our UbSRhodol data was normalized against WT (100% activity) and C878A (0% activity) (Figure 3).

Importantly, as UbSRhodol bypasses E2 enzyme requirement, mutations in the N-terminal N-lobe responsible for binding parts of an E2 distal from the E2 catalytic cysteine, hardly show an effect in our assay. However, mutations in the C-terminal C-lobe, essential for the native transthiolation, are detrimental for ligase activity. A spike in activity was observed for mutant H876A, which seems to be an artefact of the bypass system as a similar observation was made by Krist et al.^[10b] for a corresponding Rsp5 mutant. Next, we tested the ability of this set of mutants to discharge Ub from the catalytic C878 of Nedd4L by adding its cognate substrate WBP2.^[22] Since reconstituted activity of NEDD4L in vitro yields the E3~Ub adduct and some autoubiquitination product, as corroborated by bypass probe gel-based assays in the presence or absence of β ME (Supporting Information Figure 8), we observed that addition of WBP2 increased the assay window (Figure 3B) and resulted in efficient cognate substrate ubiquitination (Supporting Information Figure 9B). This set was compared to the in vitro ubiquitination of WBP2 by the native cascade using an E2~Ub discharge assay (Supporting Information Figure 9C). Fluorescence intensity read-outs of ubiquitination of WBP2 using UbSRhodol correlated with product formation ob-

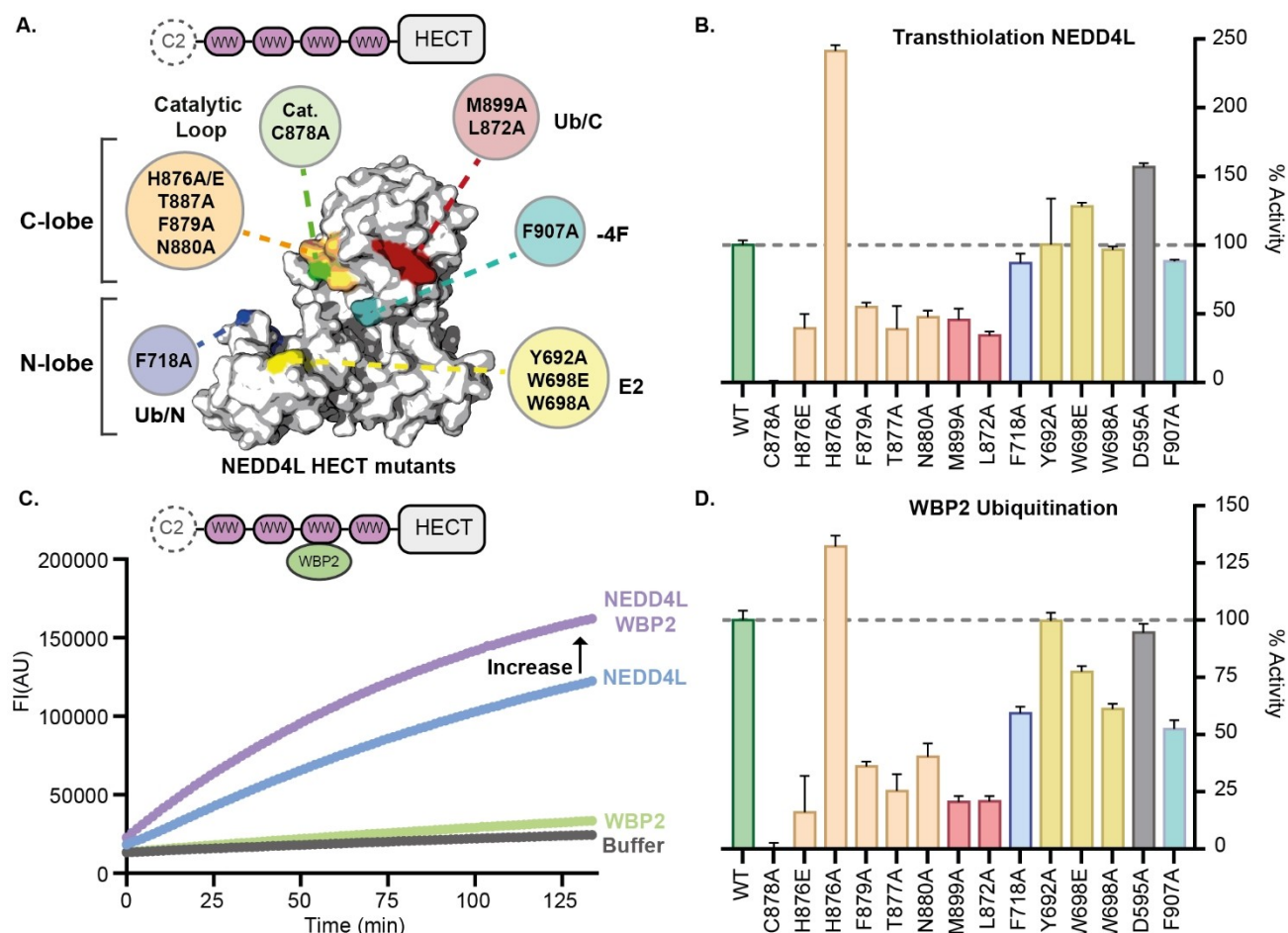


Figure 3. NEDD4L mutants and their effects on transthiolation and downstream cognate substrate ubiquitination profiled by UbSRhodol. A) Overview of Δ C2-NEDD4L HECT domain mutants derived from NEDD4L isoform 2 (PDB: Q96PU5-2). Mutations are clustered by region and depicted in green (catalytic site: C878A), orange (catalytic loop: H876A/E, T887A, F879A, N880A), blue (N-lobe Ub binding exosite: F718A), red (C-lobe Ub binding site: M899A, L872A, N880A), yellow (E2 binding site: Y692A, W698A/E), turquoise (–4F: F907A) and (not depicted) in grey (flexible linker: D595A) B) Transthiolation profile of NEDD4L. Mutants were screened against UbSRhodol under ST conditions (2.5 μ M NEDD4L vs 500 nM UbSRhodol) to measure transthiolation defects (stand. dev., $n=4$; 2 ST concentrations, 2.5 μ M and 1.25 μ M; normalized against WT (100%) and C878A (0%)). C) Ubiquitination of the model substrate WBP2 increases the assay window as WBP2 ligation results in discharge of the E3, which can then undergo multiple cycles. D) NEDD4L mediated ubiquitination of WBP2. Mutants were screened against UbSRhodol under ST conditions (2.5 μ M NEDD4L, 500 nM of WBP2 vs 500 nM UbSRhodol) to measure transthiolation defects (normalized against WT (100%) and C878A (0%)), (stand. dev., $n=4$).

served by gel-based experiments (Supporting Information Figure 9). All mutants were defective except the ones with mutations targeting the E2 binding site (W698A/E and Y692A) or Ub binding site (F718A) in the N-lobe. Hyper ubiquitination of WBP2 by H876A mutant was observed, a bypass system-dependant phenomena, as discussed above. Although the H876A mutation has decreased reactivity in the native ubiquitination cascade (Supporting Information Figure 9C), this histidine in the catalytic loop is not needed in the bypass system and might even hinder the reaction slightly. Interestingly we observed that a mutation at asparagine 880 (N880) located at the catalytic loop, was still able to ubiquitinate WBP2 in the bypass system while none was observed in the native ubiquitination. Similar to the H876A mutation, a mutation of N880 could potentially

change the positioning of the catalytic loop which decreases activity for Ub transfer with canonical E2s.

Together, our results show that UbSRhodol can be used to profile biochemical defects in transthiolation and substrate ubiquitination (ligation steps) of HECT E3s. As it utilizes an E2-independent transthiolation mechanism, caution should be taken when the mutations affect the E2 binding site. Here, the combined use with fluorescently labelled N-terminal Ub bypass probes for gel-based assays will complement the UbSRhodol readout as it facilitates discrimination between transthiolation and/or ubiquitination products.

Subsequently, we investigated if UbSRhodol could recapitulate conformational changes induced by protein-protein interactions^[6] and measure its downstream effect on ligase activity. Here we used ARIH1 and ARIH2 as these

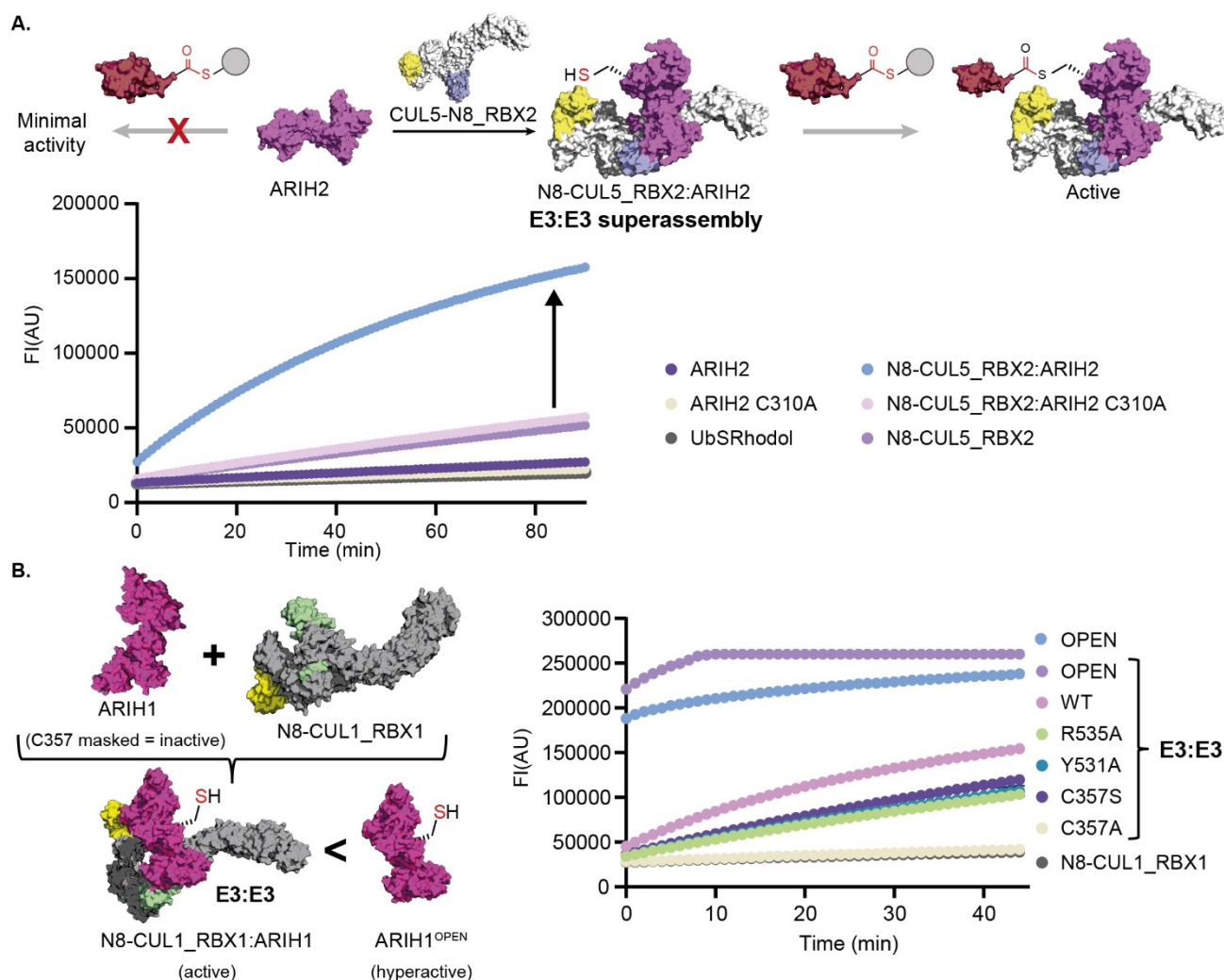


Figure 4. UbSRhodol can profile changes in activity level via E3:E3 superassembly formation of ARIH RBR ligases. A) E3:E3 superassembly of ARIH2 and neddylated CUL5:RBX2 enables transthiolation measurement overtime using UbSRhodol at ST conditions (500 nM E3:E3 superassembly and 500 nM UbSRhodol) in a plate reader. B) ARIH1 E3:E3 superassembly with neddylated CUL1:RBX1 enables profiling of different ARIH1 mutants under ST conditions (1:1:1, 500 nM). For full panel of mutants, see Supporting Information Figure 11. Note: the hyperactive mutant ARIH1^{OPEN} upon complexation with N8-CUL1-RBX1 is so active that the signal is saturated (260 k) after 10 minutes.

RBR E3 ligases possess complex autoinhibitory mechanisms.^[19] Both enzymes have autoinhibitory Ariadne domains which mask the catalytic cysteine and impede its loading from the E2~Ub. Upon complexation with neddylated Cullin-RING ligases, the ARIH Ariadne domain is sequestered and auto-inhibition concomitantly released. In this E3:E3 superassembly,^[23] the catalytic cysteine is accessible, allowing transthiolation from the E2~Ub. First, we focused on ARIH2 and investigated if we could recapitulate the activating effects of the E3:E3 superassembly^[24] formation in our assay. We compared the activity of ARIH2 alone and in complex with neddylated CUL5-RBX2 against UbSRhodol (Figure 4A). An enormous boost in ARIH2 transthiolation activity was observed when adding neddylated CUL5:RBX2 in equimolar amount. In contrast, active site mutated ARIH2 (C310A) did not show any transthiolation. These findings were corroborated by gel-based

analysis using RhoUbSR (Supporting Information Figure 10), which showed that ARIH2 wild-type (WT) is only ubiquitinated upon addition of stoichiometric amounts of neddylated CUL5:RBX2. Next, we focussed on E3-E3 complex formation of ARIH1.^[25] WT ARIH1 and relevant ligation defective mutants were assayed in the presence of neddylated CUL1-RBX1 and compared with the hyperactivated ARIH1^{OPEN} mutant.^[23a] In ARIH1^{OPEN}, the intramolecular latch between the Rcat and Ariadne domain is released by introducing three mutations in the latter (F430A, E431A, E503A), mimicking the structural reconfiguration when bound to CUL1. The “OPEN” triple mutant was in fact more active than the E3-E3 complexed WT ARIH1 in the UbSRhodol assay (Figure 3B), which was further corroborated by gel based experiments with the RhoUbSR bypass probe (Supporting Information Figure 11). Moreover, the assayed ligation defective mutants of

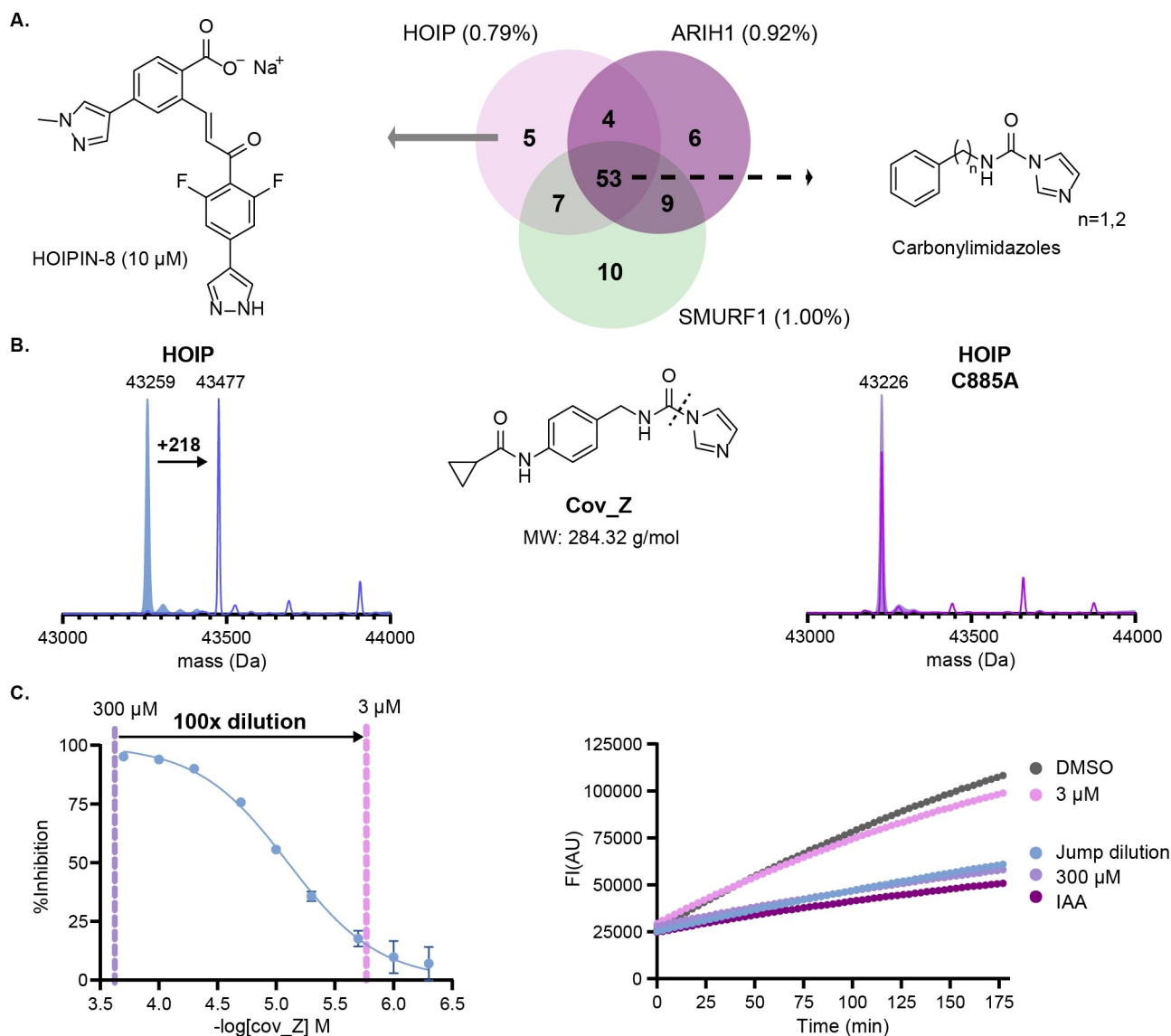


Figure 5. UbsRrhodol in a fragment-based ligand HTS screening campaign. A) Venn diagram displaying the number of validated hits (> 60% inhibition) obtained in the three screening campaigns with UbsRrhodol. Percentage indicated represents the hit rate for each E3 ligase. For a deeper characterization of compounds see Supporting Information Extended Table 1. B) MS-adduct formation experiments with carbonyl imidazole Cov_Z showed specific targeting of cysteine 885 of HOIP as confirmed by mutagenesis experiments and C) Jump dilution assays (100x dilution) against HOIP showed an irreversible covalent mode of action (showed for Cov_Z, see Supporting Information Figure 22–23 for X and Y) (stand. dev., $n = 3$).

ARIH1 showed reduced activity as recapitulated by both fluorescence intensity (Figure 3B) and gel-based read-outs (Supporting Information Figure 11C), matching previous observations.^[23a] Our data highlights that catalytic cysteine-to-alanine mutants (C357A) are preferred over cysteine-to-serine mutants (C357S) (Supporting Information Figure 11B), as the latter can still process UbsRrhodol forming an oxyster intermediate.^[26]

Collectively, this shows that our platform can detect activity changes resulting from conformational changes induced by E3–E3 super-assemblies.

A Powerful Platform for HTS

Having validated the reactivity and high sensitivity of the UbsRrhodol reagent in real time, we set out to test UbsRrhodol for High-Throughput Screening (HTS) campaigns. As a proof of concept, we employed a fragment-based ligand discovery approach to identify transthiolation blockers for three E3 ligases, namely the homologous RBR E3 ligases HOIP and ARIH1^{OPEN} and the HECT E3 ligase SMURF1, to investigate if a different subset of unique hits could be retrieved.

However, since a cysteine is targeted using electrophilic fragments and the mechanism of action of our pro-

fluorescent probe is based on cyclization of the cysteine-based linker, we first set out to investigate if commonly used positive controls in HTS, iodoacetamide (IAA) and N-ethylmaleimide (NEM) could block this cyclization progress by alkylating the thiol moiety. We titrated UbsRhodol with NEM or IAA and followed the inherent hydrolysis of the probe at pH 7.5 and pH 9 (Supporting Information Figure 12) as well as the effect of 1% DMSO. Only at high concentrations, >1 mM of IAA and >0.5 mM of NEM, or alkaline pH the cyclization process was impaired (vs 500 nM of UbsRhodol). We therefore selected 1% DMSO and 1 mM IAA as negative and positive controls respectively for our UbsRhodol screening campaigns. Here, an excess of probe over E3 ligase was chosen as MT conditions allowed screening with low E3 concentrations (Supporting Information Figure 11C, 13 and 14). The quality of our HTS assay was assessed by determining the screening window coefficient, the Z' -factor^[27] ($Z' > 0.5$ excellent). We inspected for the best balance between Z' values and amenable HTS timepoints having an acceptable assay window (Supporting Information Figure 15). In short, we decided to pick low nanomolar concentrations for HOIP (25 nM, assay window: 2–2.5 h, $Z' > 0.65$) and ARIH1^{OPEN} (15 nM, assay window 1–1.5 h, $Z' > 0.65$) and a concentration of 150 nM for SMURF1 (assay window > 2 h, $Z' = 0.7$).

We then screened HOIP (H), ARIH1^{OPEN} (A) and the HECT enzyme SMURF1 (S), lacking the C2 autoinhibitory domain, against a library of electrophilic fragments (7887 compounds, Enamine) with diverse covalent warheads and balanced reactivity (Supporting Information Figure 16) utilizing UbsRhodol. For each compound the percentage inhibition was determined from the fluorescence intensity by normalization of the measurement of the positive (iodoacetamide) and negative (DMSO) controls to 100% and 0% inhibition, respectively. Only compounds exhibiting an inhibition percentage of above 60%, were considered as hits. Next, selected hits were validated in triplicate and a different subset of unique hits was retrieved for each E3 ligase (Figure 4A and Supporting Information Extended Table 1). Here, HOIPIN-8, a known covalent inhibitor for HOIP^[28] included as positive control, was retrieved in the subset of unique hits for HOIP (Figure 5A).

Interestingly, a subset of compounds belonging to the family of carbonylimidazoles, a warhead typically reported to target serine residues,^[29] inhibited all three E3 ligases. Intrigued by their reactivity towards our ligases we tested their intrinsic reactivity in a thiol-reactivity assay. The fragments were incubated with Ellman's reagent (Supporting Information Figure 17) and no reactivity was observed towards the reagent. We next set out to assess target engagement in an orthogonal assay by measuring adduct formation by intact protein mass spectrometry (MS). Although multiple labelling was observed for ARIH1 and SMURF1 at 100 μ M (Supporting Information Figure 18 and 19), in the case of HOIP we observed mainly one modification (Figure 5B). Mutagenesis of catalytic cysteine 885 to alanine (C885A) confirmed the reactivity of these carbonylimidazoles towards cysteines (Figure 4B and Supporting Information Figure 20) as further supported by a

competition experiment with the irreversible suicide probe SulfoCy5UbVME (Supporting Information Figure 21). Here, we first incubate HOIP with the fragments after which the residual free active site cysteines are visualized by addition of SulfoCy5UbVME. A decrease in SulfoCy5UbVME-HOIP adduct, after incubation with the fragments, was observed (Supporting Information Figure 21B), corroborating our finding that these carbonylimidazoles target the catalytic cysteine of HOIP.

Although, this set of carbonylimidazole (covalent fragments X, Y and Z) require further optimization in medicinal chemistry campaigns to increase their potency and selectivity, we used them to showcase the ability of UbsRhodol to profile inhibitors. First, we assessed the IC₅₀ values of fragments X, Y and Z against HOIP (Figure 5C and Supporting Information Figure 22). Second, as potency of these fragments increased with increasing incubation time their covalent nature was assessed by jump dilution assays (Figure 5C and Supporting Information Figure 23). Our jump dilution curves (300 to 3 μ M) overlapped with the highest inhibitor concentration (300 μ M) indicating an irreversible covalent mode of action for these carbonylimidazoles X, Y and Z.

Our UbsRhodol platform allows robust HTS screening campaigns which are characterized for the low amount of E3 and substrate used, permitting screening of large libraries and conduct follow up experiments with minimal reagent.

Visualizing E3 Transthioation Activity in Cell-extract

Encouraged by the performance of UbsRhodol against recombinant proteins we set out to apply UbsRhodol in crude cell lysates. First, we explored if other members of the ubiquitination machinery could also process this thioester-based probe. For that we screened a panel of Ub enzymes of the conjugation (E1–E2–E3 (RING)) and deconjugation (DUBs and Ub-like (Ubl) proteases of SUMO and NEDD8) machinery. We observed a structural class E2^[30] dependent processing of UbsRhodol with the tested conjugation enzymes (Supporting Information Figure 24). E2 Enzymes belonging to Class I (UBE2G1, UBE2D1, UBE2D2, UBE2D3) were hardly able to process UbsRhodol, whereas members of Class III (UBE2R1 and UBE2R2) could process UbsRhodol. Next, we tested a panel of Ubl proteases as they harbor highly reactive active site cysteine residues. First, we confirmed that the proteases were active by using a well-established reagent^[31] for Ubl deconjugation enzymes based on Ub-Rho-morpholine (Supporting Information Figure 25). We then assessed potential cross-reactivity by incubating UbsRhodol with our panel of proteases (Supporting Information Figure 26). Whereas DUBs could process UbsRhodol, no cross-reactivity was observed for the Ubl proteases NEDP1 and SENP2 (Supporting Information Figure 26F, G).

Next, we overexpressed wild-type (WT) GFP-ARIH1 and different mutants WT-CS, OPEN and OPEN-CS in HEK293T cells and analysed their activity in the corresponding total cell lysates with the activity-based probe

(ABP) SCy5UbVME. In line with the assays with recombinant enzymes shown above, GFP-ARIH1 UbVME labelling activity was only observed in the ARIH1^{OPEN} expressed cell lysate (Supporting Information Figure 27). We next compared the reactivity of the activity-based probes SCy5UbVME^[32] and SCy5UbPA^[33] (with different reactive warheads) and the bypass probe (SCy5UbSR) in lysates of GFP-ARIH1^{OPEN} or -ARIH1^{OPEN-CS} expressing cells, and control cells. Labeling of GFP-ARIH1^{OPEN} was observed for both the VME-warhead ABP and the bypass probe (SR), but not for the PA-warhead probe, whereas ARIH1^{OPEN-CS} did not react at all (Figure 6A). In addition, we added UbSRhodol as substrate to these cell lysates and measured ligase dependent liberation of free Rhodol. As shown in Figure 6B (DMSO), the endogenous proteins in untransfected cells can process these type of thioester-based probes, but the activity in the lysate of GFP-ARIH1^{OPEN} but not GFP-ARIH1^{OPEN-CS} overexpressing cells was higher. Since UbSRhodol ligase recognition takes place through Ub binding domains at the catalytic domain of HECT or RBR ligases, we next included two different competitors of UbSRhodol interactions. Plain Ub76 was selected as non-covalent competitor and UbPA^[33] as putative covalent competitor and pan-inhibitor for proteases in a cell-lysate context to reduce the background since no UbPA labelling of GFP-ARIH1^{OPEN} was observed (Figure 6A). As expected, reduced processing of UbSRhodol was observed in a concentration-dependent manner, and UbPA inhibited more than Ub76 (Figure 5B and Supporting Information Figure 28). These results indicate that overexpression of active E3 ligases can offer opportunities for inhibitor profiling.

Conclusion

The enzymatic activity of Ub E3 ligases, which accommodates chemical transthiolation to alter substrates, is critical for many biological processes and can go awry, causing disease.^[34] Due to their regulatory role in cells and the recent emergence of targeted protein degradation concepts there is an increased interest in E3 ligases as drug targets.^[35] Tools for this important target class are crucial for deepening our understanding of E3 ligase biology and the discovery of new ligands for E3 ligases. Here we presented a unique reagent, UbSRhodol, to monitor Ub ligase activity, amenable to profile E3 transthiolation activity in real time. The key advantage of our methodology lies in its ability to bypass the need for E1 and E2 enzymes, its high sensitivity and ease of read-out.

Chemical synthesis of UbSRhodol, permitted us to stabilize the intrinsic reactivity of Ub-thioesters in both preparation as storage conditions. Endorsement of an auto-immolative linker onto the Ub C-terminus allowed us to profile E3 transthiolation activity by following the build-up of fluorescence intensity in real time. UbSRhodol processing by HECT/RBR E3 ligases proved catalytic cysteine-dependent at lower nanomolar concentrations among the different type and family members.

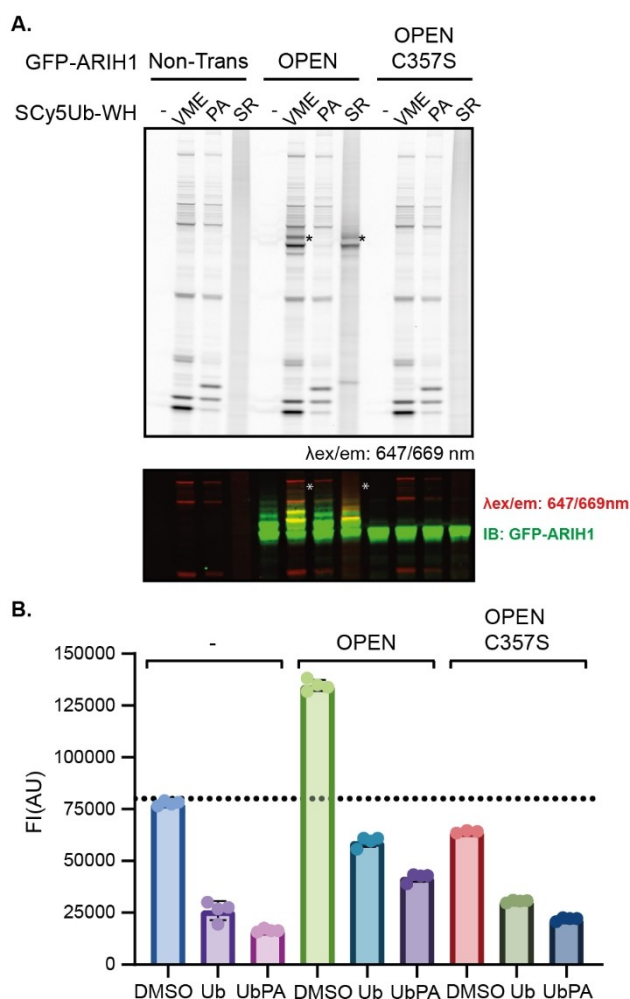


Figure 6. UbSRhodol and bypass probes to measure and visualize transthiolation activity of overexpressed E3 ligases (GFP-ARIH1). A) Reactivity of Ub based probes bearing a VME or PA electrophile warhead (WH) versus the bypass probe Ub-SR in lysates of control HEK293T cells (-) or cells overexpressing the indicated versions of GFP-ARIH1. Top: fluorescent scan after SDS-PAGE at 647/669 nm. Only GFP-ARIH1^{OPEN} containing cell lysate shows GFP-ARIH1 dependent activity with VME and SR probes (asterisk). Bottom: anti-GFP immunoblots (IB), and Cy5 fluorescent scans of the blot, corresponding to the GFP-ARIH1 containing part of the gel shown at the top. (See Supporting Information Figure 29 for full gel higher exposure and Ponceau S staining of the blot validating equal loading). B) UbSRhodol dependent transthiolation in cell lysates of control HEK293T cells (-), HEK293T cells overexpressing GFP-ARIH1^{OPEN}, or GFP-ARIH1^{OPEN-CS}. Fluorescence intensity values at time point 120 min is depicted. Experiment performed in the absence or presence of bypass probe system competitors Ub and UbPA. (stand. dev., $n=4$).

Our UbSRhodol platform provides ample possibilities for future therapeutic interventions as it allows quantitative analysis of changes in ligase activity. Not only evoked by biochemical mutations, but also by conformational changes and small molecules. Its ease of execution allows facile translation from one E3 ligase to the next, including assays for overexpressed ligases in total cell lysates, offering opportunities for E3 inhibitor screening platform in cell

lysates. Moreover, its combined use with fluorescently labelled N-terminal Ub bypass probes and/or activity-based probes for gel-based assays, as demonstrated here, complements the UbsSRhodol readout to study both transthiolation and ligation steps.

We demonstrated the robustness of our assay in an HTS setup, where we screened for small molecule modulators that block the transthiolation between our E3 enzyme and the activated Ub. In these screens we routinely achieved $Z' > 0.65$, while screening against low nanomolar E3 concentrations. Coupled to a fragment-based HTS^[36] we identified hits from a relatively small library of less complex molecules that cover the larger part of the available chemical space, thereby providing structurally diverse starting points toward E3 inhibitors and potentially increasing the repertoire of scaffolds amenable to modulate E3 ligase activity.

To properly assess inhibitor potential one does need sufficient enzyme activity, and for physiological reasons many E3 enzymes, as demonstrated here for ARIH1 and ARIH2, are for a large part present in an inhibitory conformation, inactive state, and/or complex, regulated via inhibitory domains, co-factors and/or post-translational modifications. In addition, the technical problems in reconstituting full-length HECT E3 enzymes of large HECT E3s, have urged the need for sensitive readouts, opening the avenue of in vitro activity profiling of low reactive E3 ligases constructs. As the readout of UbsSRhodol relies on unbound fluorophore only, it provides a sensitive readout that translated to a sufficient assay window enabling the study of such low reactive E3 ligases constructs, as demonstrated here for UBR5 and ARIH2 (Supporting Information Figure 30).

We anticipate that our setup will attain a thorough understanding of diseases associated with altered E3 ligase activity. Here, HECT and RBR ligases are particularly attractive drug targets, due to their key roles in various diseases,^[37] small number compared with RING ligases and their diverse domain structures that could potentially facilitate specific manipulations. UbsSRhodol can be applied as a general reagent to study E3-dependent molecular mechanisms, dissecting the contribution of e.g. protein-induced allosteric activation and substrate recognition on E3 ligase activity. Moreover, screening endeavors to scout for protein activators or inhibitors of HECT or RBR E3 ligases will open new avenues for modulation of E3 ligases activity. Based on the platform presented here we envision different ways to inhibit their activity, namely: (i) by tackling the catalytic cysteine of the enzymes; (ii) by blocking the binding of protein-protein interactions as in the context of E3:E3 superassembly formation; and (iii) by impairing substrate recognition. Additionally, these modulators can open the route towards a wide variety of chemical tools ranging from E3 specific ABPs to targeted protein degradation tools (e.g. PROTACs) targeting an E3 ligase to selectively induce protein degradation.^[38]

Author Contributions

D.A.P.B.: Conceptualization, Methodology, Investigation, Formal analysis, Validation, Visualization, Writing - Original Draft; **T.M.V.:** Investigation, Methodology, Visualization, Writing - Original Draft; **D.H.G.:** Resources, Validation, Writing - Review & Editing; **J.J.B.:** Resources, Validation, Writing - Review & Editing; **L.A.H.:** Resources, Validation, Writing - Review & Editing; **S.K.:** Resources, Writing - Review & Editing; **M.M.:** Resources, Writing - Review & Editing; **I.D.:** Resources, Writing - Review & Editing; **P.P.G.:** Formal analysis, Writing - Review & Editing; **H.D.:** Investigation, Methodology, Validation, Visualization, Writing - Original Draft, Writing - Review & Editing; **B.A.S.:** Resources, Validation, Supervision, Writing - Review & Editing; **M.P.C.M.:** Conceptualization, Methodology, Validation, Visualization, Project administration, Supervision, Writing - Original Draft, Writing - Review & Editing.

Acknowledgements

We thank Cami Talavera Ormeño for solid phase peptide synthesis and Bjorn van Doodewaerd for assistance with the ECHO screening platform. We would like to acknowledge Angeliki Moutsopoulos and Robbert Kim from the LUMC Protein Facility for molecular cloning, expression and purification of the SMURF1 proteins. We would like to acknowledge Arno Alpi from Max Planck Institute Biochemistry for plasmids of ARIH1 for cell lysate experiments. This work was supported by the European Union's Horizon 2020 research and innovation programme under the Marie Skłodowska-Curie grant agreement No. 765445 to D.P.B., the EU/EFPIA/OICR/McGill/KTH/Diamond Innovative Medicines Initiative 2 Joint Undertaking (EUOPEN grant no. 875510) and NWO (VIDI Grant VI. 213.110 to M.P.C.M.). Work in B.A.S.'s lab was funded by the ERC under the H2020 research and innovation programme (ADG-789016-Nedd8Activate), by the DFG (SCHU3196/1-1, Gottfried Wilhelm Leibniz Prize), and the Max Planck Society.

Conflict of Interest

The authors declare no conflict of interest.

Data Availability Statement

The data that support the findings of this study are available in the Supporting Information of this article.

Keywords: Biological Activity · Drug Discovery · Fluorescent Probes · E3-Ligases · Profiling Transthiolation Activity

- [1] a) A. Hershko, A. Ciechanover, *Annu. Rev. Biochem.* **1998**, *67*, 425–479; b) D. Komander, M. Rape, *Annu. Rev. Biochem.* **2012**, *81*, 203–229.
- [2] D. R. Squair, S. Virdee, *Nat. Chem. Biol.* **2022**, *18*, 802–811.
- [3] a) Y. Liao, I. Sumara, E. Pangou, *Commun. Biol.* **2022**, *5*, 114; b) C. Pohl, I. Dikic, *Science* **2019**, *366*, 818–822.
- [4] D. Popovic, D. Vucic, I. Dikic, *Nat. Med.* **2014**, *20*, 1242–1253.
- [5] I. E. Wertz, X. Wang, *Cell Chem. Biol.* **2019**, *26*, 156–177.
- [6] D. E. Spratt, H. Walden, G. S. Shaw, *Biochem. J.* **2014**, *458*, 421–437.
- [7] X. Huang, V. M. Dixit, *Cell Res.* **2016**, *27*, 484–498.
- [8] V. Landré, B. Rotblat, S. Melino, F. Bernassola, G. Melino, *Oncotarget* **2014**, *5*, 7988–8013.
- [9] R. Macarrón, R. P. Hertzberg, *Methods Mol. Biol.* **2009**, *565*, 1–32.
- [10] a) S. Park, D. T. Krist, A. V. Statsyuk, *Chem. Sci.* **2015**, *6*, 1770–1779; b) D. T. Krist, S. Park, G. H. Boneh, S. E. Rice, A. V. Statsyuk, *Chem. Sci.* **2016**, *7*, 5587–5595; c) S. Park, P. K. Foote, D. T. Krist, S. E. Rice, A. V. Statsyuk, *J. Biol. Chem.* **2017**, *292*, 16539–16553.
- [11] R. S. Kathayat, P. D. Elvira, B. C. Dickinson, *Nat. Chem. Biol.* **2017**, *13*, 150–152.
- [12] E. L. Ruggles, S. Flemer, Jr., R. J. Hondal, *Biopolymers* **2008**, *90*, 61–68.
- [13] R. R. Sauers, S. N. Husain, A. P. Piechowski, G. R. Bird, *Dyes Pigm.* **1987**, *8*, 35–53.
- [14] J. McNulty, V. Krishnamoorthy, D. Amoroso, M. Moser, *Bioorg. Med. Chem. Lett.* **2015**, *25*, 4114–4117.
- [15] R. Raz, J. Rademann, *Org. Lett.* **2011**, *13*, 1606–1609.
- [16] F. El Oualid, R. Merckx, R. Ekkebus, D. S. Hameed, J. J. Smit, A. de Jong, H. Hilkmann, T. K. Sixma, H. Ovaa, *Angew. Chem. Int. Ed.* **2010**, *49*, 10149–10153.
- [17] E. B. Getz, M. Xiao, T. Chakrabarty, R. Cooke, P. R. Selvin, *Anal. Biochem.* **1999**, *273*, 73–80.
- [18] J. Weber, S. Polo, E. Maspero, *Front. Physiol.* **2019**, *10*, 370.
- [19] a) H. Walden, K. Rittinger, *Nat. Struct. Mol. Biol.* **2018**, *25*, 440–445; b) T. R. Cotton, B. C. Lechtenberg, *Biochem. Soc. Trans.* **2020**, *48*, 1737–1750.
- [20] a) F. Wang, Q. He, W. Zhan, Z. Yu, E. Finkin-Groner, X. Ma, G. Lin, H. Li, *Structure* **2023**, *31*, 541–552.e544; b) Z. Hodáková, I. Grishkovskaya, H. L. Brunner, D. L. Bolhuis, K. Belačić, A. Schleiffer, H. Kotisch, N. G. Brown, D. Haselbach, *bioRxiv Preprint* **2022**, 2022.2011.2003.515015.
- [21] a) H. B. Kamadurai, J. Souphron, D. C. Scott, D. M. Duda, D. J. Miller, D. Stringer, R. C. Piper, B. A. Schulman, *Mol. Cell* **2009**, *36*, 1095–1102; b) J. Sluimer, B. Distel, *Cell. Mol. Life Sci.* **2018**, *75*, 3121–3141.
- [22] H. Tabatabaeian, A. Rao, A. Ramos, T. Chu, M. Sudol, Y. P. Lim, *Oncogene* **2020**, *39*, 4621–4635.
- [23] a) D. C. Scott, D. Y. Rhee, D. M. Duda, I. R. Kelsall, J. L. Olszewski, J. A. Paulo, A. de Jong, H. Ovaa, A. F. Alpi, J. W. Harper, B. A. Schulman, *Cell* **2016**, *166*, 1198–1214.e1124; b) I. R. Kelsall, D. M. Duda, J. L. Olszewski, K. Hofmann, A. Knebel, F. Langevin, N. Wood, M. Wightman, B. A. Schulman, A. F. Alpi, *EMBO J.* **2013**, *32*, 2848–2860.
- [24] S. Kostrhon, J. R. Prabu, K. Baek, D. Horn-Ghetko, S. von Gronau, M. Klügel, J. Basquin, A. F. Alpi, B. A. Schulman, *Nat. Chem. Biol.* **2021**, *17*, 1075–1083.
- [25] D. Horn-Ghetko, D. T. Krist, J. R. Prabu, K. Baek, M. P. C. Mulder, M. Klügel, D. C. Scott, H. Ovaa, G. Kleiger, B. A. Schulman, *Nature* **2021**, *590*, 671–676.
- [26] C. Garcia-Barcena, N. Osinalde, J. Ramirez, U. Mayor, *Front. Cell Dev. Biol.* **2020**, *8*, <https://doi.org/10.3389/fcell.2020.00039>.
- [27] J. H. Zhang, T. D. Chung, K. R. Oldenburg, *J. Biomol. Screening* **1999**, *4*, 67–73.
- [28] K. Katsuya, D. Oikawa, K. Iio, S. Obika, Y. Hori, T. Urashima, K. Ayukawa, F. Tokunaga, *Biochem. Biophys. Res. Commun.* **2019**, *509*, 700–706.
- [29] C. Jöst, C. Nitsche, T. Scholz, L. Roux, C. D. Klein, *J. Med. Chem.* **2014**, *57*, 7590–7599.
- [30] S. J. L. van Wijk, H. T. M. Timmers, *FASEB J.* **2010**, *24*, 981–993.
- [31] R. Kooij, S. Liu, A. Sapmaz, B. T. Xin, G. M. C. Janssen, P. A. Van Veelen, H. Ovaa, P. T. Dijke, P. P. Geurink, *J. Am. Chem. Soc.* **2020**, *142*, 16825–16841.
- [32] A. de Jong, R. Merckx, I. Berlin, B. Rodenko, R. H. M. Wijdeven, D. El Atmioui, Z. Yalçin, C. N. Robson, J. J. Neefjes, H. Ovaa, *ChemBioChem* **2012**, *13*, 2251–2258.
- [33] R. Ekkebus, S. I. Van Kasteren, Y. Kulathu, A. Scholten, I. Berlin, P. P. Geurink, A. De Jong, S. Goerdalay, J. Neefjes, A. J. R. Heck, D. Komander, H. Ovaa, *J. Am. Chem. Soc.* **2013**, *135*, 2867–2870.
- [34] a) I. Dikic, B. A. Schulman, *Nat. Rev. Mol. Cell Biol.* **2022**, *23*, 1–15; b) M. Rape, *Nat. Rev. Mol. Cell Biol.* **2018**, *19*, 59–70.
- [35] I. N. Michaelides, G. W. Collie, *J. Med. Chem.* **2023**, *66*, 3173–3194.
- [36] S. Knight, D. Gianni, A. Hendricks, *SLAS Discovery* **2022**, *27*, 3–7.
- [37] a) J. Weber, S. Polo, E. Maspero, *Front. Physiol.* **2019**, *10*, 0; b) P. Wang, X. Dai, W. Jiang, Y. Li, W. Wei, *Semin. Cancer Biol.* **2020**, *67*, 131–144; c) Y. Wang, D. Argiles-Castillo, E. I. Kane, A. Zhou, D. E. Spratt, *J. Cell Sci.* **2020**, *133*, 0, 10.1242/jcs.228072.
- [38] a) C. C. Ward, J. I. Kleinman, S. M. Brittain, P. S. Lee, C. Y. S. Chung, K. Kim, Y. Petri, J. R. Thomas, J. A. Tallarico, J. M. McKenna, M. Schirle, D. K. Nomura, *ACS Chem. Biol.* **2019**, *14*, 2430–2440; b) T. Ishida, A. Ciulli, *SLAS Discovery* **2021**, *26*, 484–502.

Manuscript received: March 6, 2023

Accepted manuscript online: June 5, 2023

Version of record online: June 27, 2023